

Towards Highly Efficient Blue-Phosphorescent Organic Light-Emitting Diodes with Low Operating Voltage and Excellent Efficiency Stability

Chunmiao Han,^[a] Guohua Xie,^[b] Hui Xu,^{*,[a]} Zhensong Zhang,^[b] Donghui Yu,^[a]
Yi Zhao,^{*,[b]} Pengfei Yan,^[a] Zhaopeng Deng,^[a] Qiang Li,^[a] and Shiyong Liu^[b]

Since the pioneering report by Forrest et al., phosphorescent organic light-emitting diodes (PHOLEDs) have been of much interest because of their ideal characteristics for highly energy-efficient, flat-panel displays and promising candidates for the next generation of solid-state lighting, such as the potential 100% internal quantum efficiency.^[1] To reduce the triplet–triplet (T–T) annihilation and concentration quenching, most of the phosphorescent dyes of heavy-metal complexes are doped in host materials to improve the device performance.^[2] Nevertheless, stable and efficient blue PHOLEDs remain a significant challenge.^[3] In the host–guest doping of blue electrophosphorescent devices, the efficient positive energy transfer to the guest requires a very high first triplet energy level (T_1) of the host (approaching 3.0 eV).^[4] Usually, a host with a high triplet energy level exhibits a high driving voltage due to poor carrier-transporting properties originating from the intrinsic wide band gap. For practical use, the low operating voltage is another significant indicator, which requires fitting of the frontier molecular orbitals (FMOs) of the host and the neighbouring carrier-transporting layers. It indicates that the low first singlet energy level (S_1) of the host can decrease the driving voltage of OLEDs.^[5] Therefore, development of host materials with both high T_1 and relatively low S_1 be-

comes one of the critical points for high-performance blue PHOLEDs.

Most of the hosts with high T_1 are designed with the incorporation of *meso* or insulating linkages, such as *N,N*-dicarbazoly-3,5-benzene (mCP)^[4] and tetraaryl silane derivatives.^[6] However, the operating voltages of the devices remain high (≈ 10 V at practical luminance). The high LUMO of mCP (2.4 eV) and the electrical inertia of silicon are the main factors for the high driving voltages.^[7a] Recently, hosts based on aryl phosphine oxides (APO) have attracted intensive interest.^[7] The phosphine oxide moieties are believed to efficiently polarise the molecules without extending the conjugated length of the active chromophore.^[7b] Such characteristics make APOs obtain good carrier-injection/transporting abilities and, at the same time, retain high T_1 levels. Nevertheless, only a few blue PHOLEDs based on APO hosts exhibit low driving voltages (< 5 V) and low efficiency roll-offs ($< 30\%$) at a practical luminance of 1000 cd m^{-2} .^[5,7a,d,e] Nearly all of the APO hosts reported have diphenylphosphine oxide (DPPO) moieties substituting the chromophores along the long axis of the molecules, such as 2,7-substitution of fluorene,^[7b,f-h] 3,6-substitution of carbazole^[7a] and 2,8-substitution of dibenzofuran.^[7c] Such symmetrical structures are unfavourable to retain T_1 and efficiently polarising the chromophores.

Although only a few hosts are designed with the *ortho* linkage,^[8,7f] this modification is advantageous in the construction of high-performance blue-electrophosphorescent APO hosts because 1) the *ortho*-linked phosphine oxide facilitates the retention of T_1 ; 2) through *ortho* substitution, the DPPO moieties are on the short axis of the chromophores; this facilitates the polarisation of the chromophores and 3) the unsymmetrical structure of the *ortho* linkage would suppress intermolecular aggregation and further limit the efficiency roll-off at high luminance.

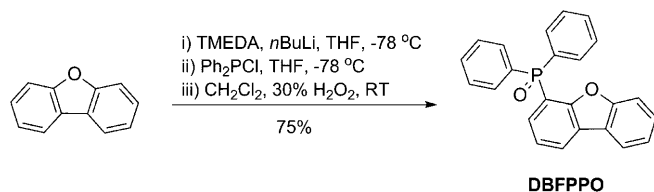
Herein, we report a novel dibenzofuran phosphine oxide host, 4-diphenylphosphoryl dibenzofuran (*o*-DBFPPO), which is formed through *ortho* linkage of dibenzofuran and a DPPO moiety. Low driving voltages (3.1 V at 100 cd m^{-2})

[a] C. Han, Dr. H. Xu, D. Yu, Prof. P. Yan, Z. Deng, Dr. Q. Li
Key Laboratory of Functional Inorganic Material Chemistry
Ministry of Education, Heilongjiang University
74 Xuefu Road, Harbin 150080 (P.R. China)
Fax: (+86) 451-86608042
E-mail: hxu@hlju.edu.cn

[b] G. Xie, Z. Zhang, Prof. Y. Zhao, Prof. S. Liu
State Key Laboratory on Integrated Optoelectronics
College of Electronics Science and Engineering
Jilin University, 2699 Qianjin Street, Changchun 130012 (P.R. China)
Fax: (+86) 431-5095592
E-mail: zhao_yi@jlu.edu.cn

Supporting information for this article is available on the WWW under <http://dx.doi.org/10.1002/chem.201001981>.

and low efficiency roll-offs (4% external quantum efficiency (EQE) for 100–1000 cdm^{-2}) of the corresponding blue PHOLEDs were demonstrated. *o*-DBFPPO was conveniently prepared through a three-step procedure of regioselective lithiation, coupling to the phosphine and oxidation, with a good total yield over 70% (Scheme 1). The structural char-



Scheme 1. Synthesis of *o*-DBFPPO. TMEDA = *N,N,N',N'*-tetramethylethylenediamine.

acterisation was established on the basis of mass spectrometry, NMR spectroscopy and elemental analysis (see the Supporting Information). The molecular structure was further confirmed by X-ray crystallography (Figure 1).^[9] Because of the hindrance of the *ortho* linked DPPO, no π - π stacking between neighbouring *o*-DBFPPO molecules is observed (Figure S1 in the Supporting Information), in contrast to the *para*-linked dibenzofuran phosphine oxide derivatives.^[7c] Thus, the *ortho* linkage has a remarkable effect on reducing intermolecular interactions.

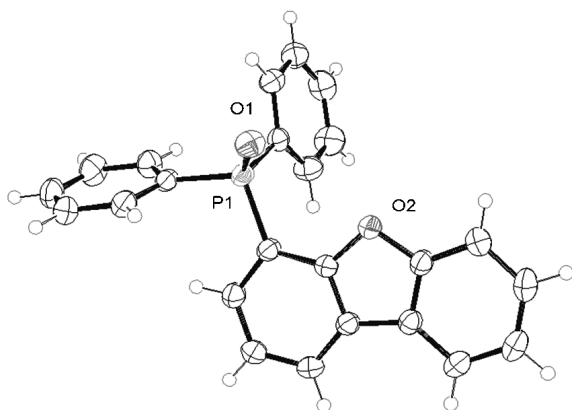


Figure 1. ORTEP diagram of *o*-DBFPPO with thermal ellipsoids of 30% probability.

The thermal properties of *o*-DBFPPO were investigated by thermogravimetric analysis (TGA) and differential scanning calorimetry (DSC). The decomposition temperature (T_d) of DBFPPO is 296 °C, which makes the fabrication of the device feasible through vacuum evaporation. The DSC result shows that *o*-DBFPPO has a melting point (T_m) of 188 °C. The temperature of the glass transition (T_g) of DBFPPO is about 89 °C, which is much higher than that of mCP (60 °C). The higher T_g may be attributed to the more compact structure of *o*-DBFPPO because of the *ortho* link-

age. The improved thermal properties of *o*-DBFPPO enhance the stability of the film morphology and suppress the potential phase separation during operation.

The more efficient polarisation of dibenzofuran by the *ortho* linkage of DPPO was proved by DFT calculations of *o*-DBFPPO and its *para*-linked isomer, *p*-DBFPPO. The structure optimisation was performed by using the Gaussian 03 package at the B3LYP 6-31G* level.^[10] The calculated HOMOs of *o*-DBFPPO and *p*-DBFPPO are -6.15 and -6.20 eV, respectively, whereas the calculated LUMOs of *o*-DBFPPO and *p*-DBFPPO are -1.20 and -1.15 eV, respectively (Figure 2). The HOMO-LUMO energy gap (E_g) of *o*-

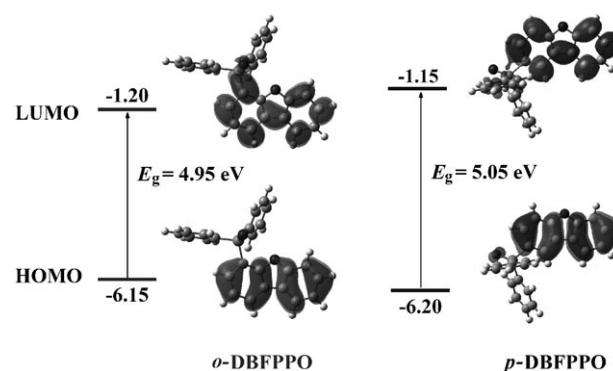


Figure 2. DFT calculation results of *o*-DBFPPO and *p*-DBFPPO.

DBFPPO is 4.95 eV, which is 0.1 eV smaller than that of *p*-DBFPPO. With the lower LUMO and higher HOMO, *o*-DBFPPO is expected to be more predominant in carrier injection and transporting than *p*-DBFPPO. Although all of the FMO electron clouds are mainly located on dibenzofuran, the LUMO and HOMO electron cloud distributions of the two compounds are very different. For *p*-DBFPPO, *para* substitution of electron-withdrawing DPPO does not affect the uniform distribution of the FMO electron cloud on dibenzofuran. However, for *o*-DBFPPO, the phenyl linking makes a major contribution to the LUMO, but only a minor contribution to the HOMO (Figure 2). It means that dibenzofuran is bipolarised to some degree by the *ortho* linkage of DPPO. This facilitates the balance of carrier injection and transporting in the emitting layer (EML). The LUMO and HOMO energy levels of *o*-DBFPPO were further determined by cyclic voltammetry (CV) to have values of -2.86 and -5.96 eV, respectively.

The absorption and fluorescence spectra of *o*-DBFPPO in films and dilute solutions are shown in Figure 3. The absorptions at around 290 nm are attributed to $\pi \rightarrow \pi^*$ transitions of dibenzofuran. This band is enhanced in films due to the π - π interaction between neighbouring dibenzofurans. The first singlet excited energy level (S_1) of *o*-DBFPPO is 3.89 eV estimated from the absorption edge (319 nm). The photoluminescence (PL) emission of *o*-DBFPPO at room temperature is in the range of 300–415 nm with a maximum intensity at 326 nm, which is thoroughly overlapped with the

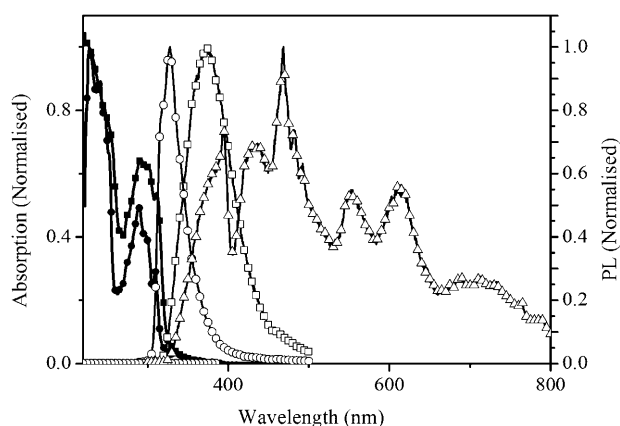


Figure 3. Absorption and emission spectra of *o*-DBFPPO in a film and in CH_2Cl_2 ($1 \times 10^{-5} \text{ M}$) and phosphorescence spectrum of *o*-DBFPPO in CH_2Cl_2 ($1 \times 10^{-5} \text{ M}$) at 77 K: ■: absorption in the film, ●: absorption in CH_2Cl_2 , □: emission in the film, ○: emission in CH_2Cl_2 and △: phosphorescence in CH_2Cl_2 .

metal-to-ligand charge-transfer (MLCT) absorption peak of the blue-phosphorescent-emitting bis(4,6-(difluorophenyl)pyridinato-*N,C2*)picolinatoiridium(III) (FIrpic) constituting the basis of the diode. The phosphorescence spectrum of *o*-DBFPPO was also measured at 77 K. T_1 of *o*-DBFPPO estimated from the $\nu_{0,0}$ transition identified as the highest-energy band (394 nm) was as high as 3.15 eV, which was 0.4 eV higher than that of FIrpic (2.75 eV). Therefore, an efficient exothermic energy transfer from *o*-DBFPPO to FIrpic can be expected. Simultaneously, the energy gap between S_1 and T_1 (ΔE_{ST}) of *o*-DBFPPO is only 0.74 eV. The small ΔE_{ST} reduces the driving voltage of PHOLEDs.^[5]

To investigate the performance of *o*-DBFPPO as the host material, three I-type devices (device I-A, I-B and I-C) were fabricated through vacuum evaporation with the same configuration of ITO/MoO_x (2 nm)/*m*-MTDATA: MoO_x (3:1, 10 nm)/*m*-MTDATA (30 nm)/[Ir(ppz)₃] (10 nm)/*o*-DBFPPO: FIrpic (10:1, *x* nm)/BPhen ((50−*x*) nm)/LiF (1 nm)/Al (for I-A, *x*=10; for I-B, *x*=20; for I-C, *x*=30), in which MoO_x and LiF served as hole- and electron-injecting layers, *m*-MTDATA is 4,4',4''-tri(*N*-3-methylphenyl-*N*-phenylamino)-triphenylamine, which served as a hole-transporting layer (HTL), BPhen is 4,7-diphenyl-1,10-phenanthroline, which served as an electron-transporting layer (ETL), and [Ir(ppz)₃] is tris(phenylpyrazole)iridium, which was used as both hole-transporting and electron-blocking materials, respectively. The combined thickness of EML and ETL was 50 nm. Therefore, from I-A to I-C, the thickness of EML increased from 10 to 30 nm, whereas the thickness of the ETL decreased from 40 to 20 nm. Device I-A showed the lowest turn-on voltage of 2.6 V at 3 cd m^{−2}, and the driving voltages at 100 and 1000 cd m^{−2} were as low as 3.1 and 4.0 V, respectively (Figure 4a). These are the lowest operating voltages reported so far among the single-host/FIrpic-based PHOLEDs.^[5,7] Along with increasing thickness of the EML, the driving voltages also gradually increased, which implies that the electron-injection/transporting ability of *o*-DBFPPO is

weaker than that of BPhen. Although among the I-type devices I-B showed the highest efficiency of 28 Lm W^{−1} (30 cd A^{−1}, 13.3%) at 90 cd m^{−2} (Figure 4c and Figure S4 in the Supporting Information), device I-A exhibited the most stable efficiency between 100–1000 cd m^{−2}, the percentages of efficiency roll-off are only 23% for power efficiency (PE), 4% for current efficiency (CE) and 4% for EQE. To the best of our knowledge, this is among the highest levels reported for single-host/FIrpic-based PHOLEDs and comparable to mixed-host-based devices.^[5,7g,h]

Because FIrpic and BPhen have similar T_1 values ($T_1 = 2.78$ eV), the electron-transporting tri[3-(3-pyridyl)mesityl]borane (3TPYMB), which has a much higher T_1 value (2.95 eV), was inserted between the EML and BPhen layers as exciton-blocking layer to prevent the diffusion of T_1 exciton from EML to ETL. This led to the construction of four II-type devices (device II-A, II-B, II-C and II-D), the configurations of which were ITO/MoO_x (2 nm)/*m*-MTDATA: MoO_x (3:1, 10 nm)/*m*-MTDATA (30 nm)/[Ir(ppz)₃] (10 nm)/DBFPPO:FIrpic (10:1, 10 nm)/3TPYMB (*y* nm)/BPhen ((40−*y*) nm)/LiF(1 nm)/Al (for II-A, *y*=0; for II-B, *y*=5; for II-C, *y*=10; for II-D, *y*=15). The combined thickness of 3TPYMB and BPhen was 40 nm. Therefore, from II-A to II-D, the thickness of the 3TPYMB layer increased from 0 to 15 nm, whereas the thickness of the BPhen layer decreased from 40 to 25 nm. Devices II-A and II-B showed similar current–voltage characteristics. The driving voltages of II-C and II-D gradually increased compared with II-A and II-B; this may be attributed to the strong hole-blocking ability of 3TPYMB (HOMO = −6.77 eV) (Figure 4b). Because of the efficient T_1 exciton blocking, the highest CE and EQE values of II-C (139 cd m^{−2}) were improved to 35.5 cd A^{−1} and 15.5%, respectively. However, with the lower operating voltage, device II-B showed the highest PE of 36 Lm W^{−1} at 83 cd m^{−2} (Figure 4d and Figure S5 in the Supporting Information). Simultaneously, device II-B had the most stable efficiencies among the II-type devices with very low efficiency roll-offs of 25% for PE, 9% for CE and 9% for EQE (100–1000 cd m^{−2}).

The electroluminescent (EL) spectra of the I- and II-type devices at 1000 cd m^{−2} are shown in Figure 4a and b. The main peaks appear at 468 nm. The shoulder peaks at 500 nm are much weaker. The Commission Internationale de L'Eclairage (CIE) coordinates are (0.16, 0.32) and (0.15, 0.29) for the I- and II-type devices, respectively. These coordinates are remarkably smaller than for other PHOLEDs based on phosphine oxide hosts and FIrpic.^[7b–h] The vibrational peak at 500 nm is attributed to the recombination zones close to the interfaces between carrier-transporting layers and EMLs.^[7h] The *ortho* linkage endows *o*-DBFPPO with both hole- and electron-injection/transporting abilities, which induce the recombination zones to shift to the centre of EML and further reduce the vibrational peaks. The more efficient polarisation of dibenzofuran in *o*-DBFPPO is also the reason for the extremely stable EL efficiencies of the I- and II-type devices. For most phosphine oxide hosts, stronger electron-injection/transporting ability leads limitations

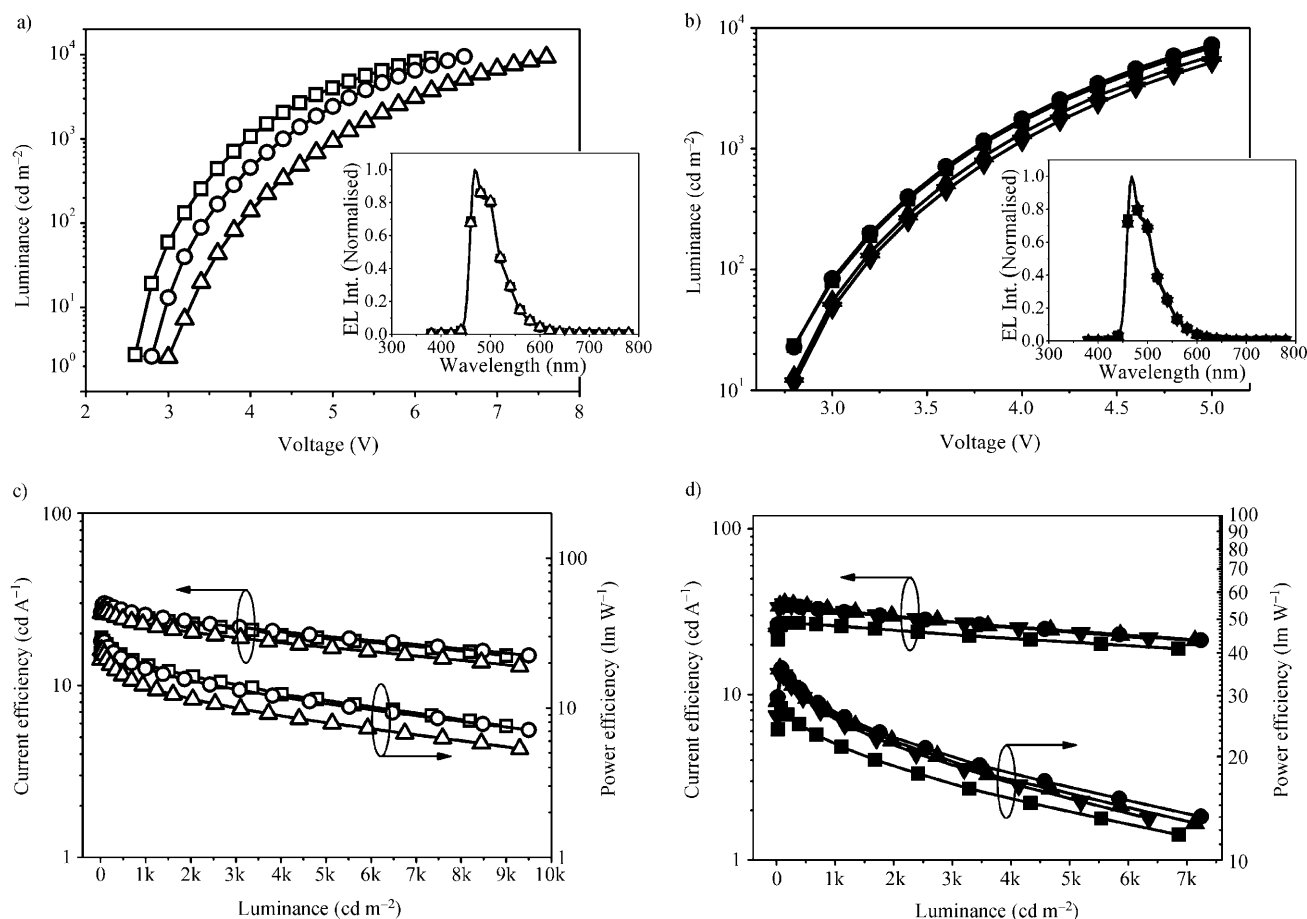


Figure 4. a) Voltage–luminance characteristics of I-type devices (\square : I-A; \circ : I-B and \triangle : I-C), and their EL spectra at 1000 cd m^{-2} (inset). b) Voltage–luminance characteristics of II-type devices (\blacksquare : II-A, \bullet : II-B, \blacktriangle : II-C, \blacktriangledown : II-D), and their EL spectra at 1000 cd m^{-2} (inset). c) Luminance–efficiency curves of I-type devices (\square : I-A, \circ : I-B and \triangle : I-C). d) Luminance–efficiency curves of II-type devices (\blacksquare : II-A, \bullet : II-B, \blacktriangle : II-C and \blacktriangledown : II-D).

of the recombination zone to a narrow zone close to the HTL side. The balanced carrier-injection/transporting ability of *o*-DBFPPO expanded the recombination zone to the bulk of EML, instead of the interfaces. Therefore, the exciton concentration quenching and triplet–triplet annihilation were reduced in the I- and II-type devices at high luminance.

Table 1 lists the EL performance of several representative Firpic-based PHOLEDs. Compared with *o*-DBFPPO the related *para*-linked 2,8-bis(diphenylphosphine oxide)dibenzofuran (2,8-DBFDPPPO) shows lower maximum efficiencies (20.1 lm W^{-1} and 20.2 cd A^{-1}), worse efficiency roll-off (65% for PE and 39% for CE at 800 cd m^{-2}) and higher operating voltages (3.3 V onset and 5.6 V at 800 cd m^{-2}).^[7c] The state-of-the-art efficiency stability, high

colour purity and low operating voltage make *o*-DBFPPO one of the most effective hosts for blue PHOLEDs.

In summary, an effective strategy for the design of highly efficient phosphine oxide hosts with an *ortho*-linked structure has been demonstrated by a simple dibenzofuran phosphine oxide host. The *ortho* linkage of the DPPO moiety has the dual effect of retaining the high T_1 and efficiently

Table 1. EL performance of representative Firpic-based devices.

Host ^[a]	Driving voltage [V]	Max. efficiency ^[b]	Efficiency roll-off [%] ^[b]	CIE (x, y)
2,8-DBFDPPPO ^[7c]	3.3, ^[c] 5.6 ^[d]	20.1, 20.2, –	65, 39, – ^[d]	–, –
PCF ^[7d]	2.6, ^[c] 4.3 ^[e]	26.2, 30.8, 14.8	25, 13, 13 ^[e]	0.13, 0.35
BCBP ^[5c]	3.0, ^[c] 4.8, ^[f] 7.0 ^[e]	47, 50, 22	35, –, 10 ^[f]	–, –
SPPO1 ^[7h]	3.0, ^[c] 6.1 ^[e]	28, –, 11.5	70, –, 40 ^[e]	0.195, 0.438
SPPO11 ^[7f]	3.5, ^[c] 5.5 ^[e]	24.7, 35.6, 17.5	27, –, 5 ^[e]	–, –
BCPO ^[7g]	2.8 ^[c]	40.6, 45.1, 23.5	–, –, 18 ^[c]	–, –
CzTP ^[5a]	3.0, ^[c] 3.4, ^[f] 4.1 ^[e]	55, 52, –	47, 27, – ^[e]	–, –
CzSi ^[6b]	3.0, ^[c] 5.0, ^[f] ≈ 7.0 ^[e]	26.7, 30.6, 15.7	40, 22, 24 ^[f]	–, –
<i>o</i> -DBFPPO	2.6, ^[c] 3.1, ^[f] 4.0 ^[e]	36, 35.5, 15.5	23, 4, 4 ^[c]	0.15, 0.29

[a] PCF = 2,7-bis(diphenylphosphine oxide)-9-(9-phenylcarbazol-3-yl)-9-phenylfluorene, BCBP = 2,20-bis(4-carbazolylphenyl)-1,10-biphenyl, SPPO1 = 2-(diphenylphosphoryl)spirofluorene, SPPO11 = 4-(diphenylphosphoryl)spirofluorene, BCPO = bis-4-(*N*-carbazolyl)phenylphenylphosphine oxide, CzTP = 9-phenyl-3,6-bis-[1,1':3'1'']terphenyl-5'-yl-9*H*-carbazole, CzSi = 9-(4-*tert*-butylphenyl)-3,6-bis(triphenylsilyl)-9*H*-carbazole. [b] Appearing in the following order: PE [lm W^{-1}], CE [cd A^{-1}] and EQE [%]. [c] Onset voltage. [d] At 800 cd m^{-2} . [e] At 1000 cd m^{-2} . [f] At 100 cd m^{-2} .

polarising the chromophores. As a result, the blue *o*-DBFPPO-based PHOLEDs showed superior performance with low driving voltages (3.1 V at 100 cd m⁻²), low efficiency roll-offs (4% for EQE 100–1000 cd m⁻²) and high colour purity ($x + y < 0.45$).

Acknowledgements

This work was financially supported by the National Key Basic Research and Development Program of China under grant no. 2010CB327701, NSFC under Grant 50903028 and 60977024, Natural Science Foundation of Heilongjiang province under Grant QC08C10, the Supporting Program of Innovation teams of HLJU (hdt2010-08), HLJU Funds for Distinguished Young Teachers and Education Bureau of Heilongjiang province under grant 2010td03.

Keywords: density functional calculations • doping • fluorescence • light-emitting diodes • phosphorus

- [1] M. A. Baldo, D. F. O'Brien, Y. You, A. Shoustikov, S. Sibley, M. E. Thompson, S. R. Forrest, *Nature* **1998**, *395*, 151–154.
- [2] S. Reineke, F. Lindner, G. Schwartz, N. Seidler, K. Walzer, B. Lussem, K. Leo, *Nature* **2009**, *459*, 234–238.
- [3] a) M. A. Baldo, S. Lamansky, P. E. Burrows, M. E. Thompson, S. R. Forrest, *Appl. Phys. Lett.* **1999**, *75*, 4–6; b) C. Adachi, R. C. Kwong, P. Djurovich, V. Adamovich, M. A. Baldo, M. E. Thompson, S. R. Forrest, *Appl. Phys. Lett.* **2001**, *79*, 2082–2084; c) S. Beaupré, P.-L. T. Boudreault, M. Leclerc, *Adv. Mater.* **2010**, *22*, E6-E27; d) K. T. Kamtekar, A. P. Monkman, M. R. Bryce, *Adv. Mater.* **2010**, *22*, 572–582; e) K. T. Kamtekar, H. L. Vaughan, B. P. Lyons, A. P. Monkman, S. U. Pandya, M. R. Bryce, *Macromolecules* **2010**, *43*, 4481–4488.
- [4] R. J. Holmes, S. R. Forrest, Y.-J. Tung, R. C. Kwong, J. J. Brown, S. Garon, M. E. Thompson, *Appl. Phys. Lett.* **2003**, *82*, 2422–2424.
- [5] a) H. Sasabe, Y.-J. Pu, K. Nakayama, J. Kido, *Chem. Commun.* **2009**, 6655–6657; b) S.-J. Su, E. Gonmori, H. Sasabe and J. Kido, *Adv. Mater.* **2008**, *20*, 4189–4194; c) L. X. Xiao, S.-J. Su, Y. Agata, H. Lan, J. Kido, *Adv. Mater.* **2009**, *21*, 1271–1274.
- [6] a) X. Ren, J. Li, R. J. Holmes, P. I. Djurovich, S. R. Forrest, M. E. Thompson, *Chem. Mater.* **2004**, *16*, 4743–4747; b) M.-H. Tsai, H.-W. Lin, H.-C. Su, T.-H. Ke, C.-C. Wu, F.-C. Fang, Y.-L. Liao, K.-T. Wong, C.-I. Wu, *Adv. Mater.* **2006**, *18*, 1216–1220.
- [7] a) S. O. Jeon, K. S. Yook, C. W. Joo, J. Y. Lee, *Adv. Funct. Mater.* **2009**, *19*, 3644–3649; b) A. B. Padmaperuma, L. S. Sapochak, P. E. Burrows, *Chem. Mater.* **2006**, *18*, 2389–2396; c) P. A. Vecchi, A. B. Padmaperuma, H. Qiao, L. S. Sapochak, P. E. Burrows, *Org. Lett.* **2006**, *8*, 4211–4214; d) F.-M. Hsu, C.-H. Chien, P. I. Shih, C. F. Shu, *Chem. Mater.* **2009**, *21*, 1017–1022; e) E. Polikarpov, J. S. Swensen, N. Chopra, F. So, A. B. Padmaperuma, *Appl. Phys. Lett.* **2009**, *94*, 223304(1–3); f) S. E. Jang, C. W. Joo, S. O. Jeon, K. S. Yook, J. Y. Lee, *Org. Electron.* **2010**, *11*, 1059–1065; g) J. Lee, J.-I. Lee, J. Y. Lee, H. Y. Chu, *Appl. Phys. Lett.* **2009**, *95*, 253304; h) J. Lee, J. I. Lee, J. Y. Lee, H. Y. Chu, *Org. Electron.* **2009**, *10*, 1529–1533; i) H.-H. Chou, C.-H. Cheng, *Adv. Mater.* **2010**, *22*, 2468–2471.
- [8] Y. T. Tao, Q. Wang, C. L. Yang, Q. Wang, Z. Q. Zhang, T. T. Zou, J. G. Qin, D. G. Ma, *Angew. Chem.* **2008**, *120*, 8224–8227; *Angew. Chem. Int. Ed.* **2008**, *47*, 8104–8107.
- [9] CCDC-802231 contains the supplementary crystallographic data for this paper. These data can be obtained free of charge from The Cambridge Crystallographic Data Centre via www.ccdc.cam.ac.uk/data_request/cif.
- [10] Gaussian 03, Revision D.02, M. J. Frisch, G. W. Trucks, H. B. Schlegel, G. E. Scuseria, M. A. Robb, J. R. Cheeseman, J. A. Montgomery, Jr., T. Vreven, K. N. Kudin, J. C. Burant, J. M. Millam, S. S. Iyengar, J. Tomasi, V. Barone, B. Mennucci, M. Cossi, G. Scalmani, N. Rega, G. A. Petersson, H. Nakatsuji, M. Hada, M. Ehara, K. Toyota, R. Fukuda, J. Hasegawa, M. Ishida, T. Nakajima, Y. Honda, O. Kitao, H. Nakai, M. Klene, X. Li, J. E. Knox, H. P. Hratchian, J. B. Cross, V. Bakken, C. Adamo, J. Jaramillo, R. Gomperts, R. E. Stratmann, O. Yazyev, A. J. Austin, R. Cammi, C. Pomelli, J. W. Ochterski, P. Y. Ayala, K. Morokuma, G. A. Voth, P. Salvador, J. J. Dannenberg, V. G. Zakrzewski, S. Dapprich, A. D. Daniels, M. C. Strain, O. Farkas, D. K. Malick, A. D. Rabuck, K. Raghavachari, J. B. Foresman, J. V. Ortiz, Q. Cui, A. G. Baboul, S. Clifford, J. Ciołowski, B. B. Stefanov, G. Liu, A. Liashenko, P. Piskorz, I. Komaromi, R. L. Martin, D. J. Fox, T. Keith, M. A. Al-Laham, C. Y. Peng, A. Nanayakkara, M. Challacombe, P. M. W. Gill, B. Johnson, W. Chen, M. W. Wong, C. Gonzalez, J. A. Pople, Gaussian, Inc., Wallingford CT, **2004**.

Received: July 13, 2010
Published online: December 3, 2010